JCB Article

A mutant heterodimeric myosin with one inactive head generates maximal displacement

Neil M. Kad, Arthur S. Rovner, Patricia M. Fagnant, Peteranne B. Joel, Guy G. Kennedy, Joseph B. Patlak, David M. Warshaw, and Kathleen M. Trybus

Department of Molecular Physiology and Biophysics, University of Vermont, Health Science Research Facility, Burlington, VT 05405

Each of the heads of the motor protein myosin II is capable of supporting motion. A previous report showed that double-headed myosin generates twice the displacement of single-headed myosin (Tyska, M.J., D.E. Dupuis, W.H. Guilford, J.B. Patlak, G.S. Waller, K.M. Trybus, D.M. Warshaw, and S. Lowey. 1999. *Proc. Natl. Acad. Sci. USA.* 96:4402–4407). To determine the role of the second head, we expressed a smooth muscle heterodimeric heavy meromyosin (HMM) with one wild-type head, and the other locked in a weak actin-binding state by introducing a point mutation in switch II (E470A). Homodimeric E470A HMM did not support in vitro motility, and only slowly hydrolyzed MgATP. Optical trap measurements revealed that the heterodimer generated unitary displacements of 10.4 nm, strikingly similar to wild-type HMM (10.2 nm) and approximately twice that of single-headed subfragment-1 (4.4 nm). These data show that a double-headed molecule can achieve a working stroke of ~10 nm with only one active head and an inactive weak-binding partner. We propose that the second head optimizes the orientation and/or stabilizes the structure of the motion-generating head, thereby resulting in maximum displacement.

Introduction

Muscle myosin II is a hexameric molecular motor composed of two identical heavy chains, each noncovalently associated with two light chains. At the NH_2 terminus of each heavy chain is a globular "head" that contains the ATP- and actin-binding sites, followed by the light chain binding domain or "neck" that acts as a lever arm (Rayment et al., 1993). It is widely believed that rotation of this lever results in the displacement of actin (Huxley and Kress, 1985; Uyeda et al., 1996; Baker et al., 1998; Dominguez et al., 1998; Corrie et al., 1999; Houdusse et al., 2000; Shih and Spudich, 2001).

Whether myosin's two heads act independently or cooperatively is a question that remains open, with evidence favoring both points of view (Margossian and Lowey, 1973, 1978; Cooke and Franks, 1978; Harada et al., 1987; Toyoshima et al., 1987; Cremo et al., 1995; Conibear and Geeves, 1998; Katayama, 1998; Ito et al., 1999). At the single-molecule level, it was shown that double-headed myosin produced twice the unitary displacement and twice the force of single-headed myosin (Tyska et al., 1999). The time that myosin remained attached to actin after the power stroke was the same for both species, leading to the hypothesis that motion generation originated from only one of the two heads. We proposed that the second head guided the first to its maximal displacement.

To test this hypothesis further and to determine what features of the second head are required for motion generation, we expressed a heterodimeric smooth muscle heavy meromyosin (HMM) with two functionally different heads. This heterodimer is composed of one wild-type head and the other locked in a weak actin-binding state, through the introduction of a point mutation in switch II (E470A) of the nucleotide-binding site (Sasaki et al., 1998; Kojima et al., 1999). When myosin is in a conformation that is competent to hydrolyze MgATP, E470 forms a salt bridge with R247 in switch I.

Here, we show that the double-headed heterodimer with only one active head produces the same step size as wild-type HMM (wt-HMM) with two active heads, and twice that of

N.M. Kad and A.S. Rovner contributed equally to this paper.

Address correspondence to David M. Warshaw, Dept. of Molecular Physiology and Biophysics, University of Vermont, Health Science Research Facility, Burlington, VT 05405-0068. Tel.: (802) 656-2540. Fax: (802) 656-0747. email: warshaw@physiology.med.uvm.edu; or Kathleen M. Trybus, Dept. of Molecular Physiology and Biophysics, University of Vermont, Health Science Research Facility, Burlington, VT 05405-0068. Tel.: (802) 656-8750. Fax: (802) 656-0747. email: trybus@physiology.med.uvm.edu

Key words: step size; single molecule; optical trap; molecular motor; cooperativity

Abbreviations used in this paper: FPLC, fast performance liquid chromatography; HMM, heavy meromyosin; Pyr-actin, pyrene-labeled actin; S1-neo, single-headed subfragment-1 with neonatal epitope tag; wt-HMM, wild-type heavy meromyosin.

an expressed single-headed S1 construct. This result confirms that only one of the two heads displaces actin, and that the presence of a second head is necessary for the motion-generating head to produce its maximal displacement. The mechanism by which the second head exerts its influence could either be through its weak association with actin, or by stabilizing the head–rod junction and minimizing unfavorable orientations of the working head. Regardless of mechanism, these experiments establish that myosin's second head plays a critical role in maximizing the distance actin is moved per cycle of ATP hydrolysis.

Results

The E470A mutant has a long-lived weakly bound state

To determine the role of each head in actin movement, we engineered a mutant heterodimeric HMM with one wild-type cycling head and one inactive weak-binding head, which was achieved by introducing a point mutation in switch II (E470A). The homodimeric E470A-HMM was first characterized to confirm the predominant biochemical state of the mutant head (Onishi et al., 1998a,b; Suzuki et al., 1998). When nucleotide-free phosphorylated E470A-HMM (see Materials and methods) was added to pyrene-labeled actin (Pyr-actin), it caused a large decrease in fluorescence (Fig. 1 A), indicating that the mutant can isomerize to the strong binding state (Criddle et al., 1985). Addition of ATP to ~0.4 mol/mol of HMM caused a rapid increase in fluorescence, followed by a slow decay that was fit to a single exponential with a rate constant of ~0.0004 s^{-1} (Fig. 1 A). Therefore, E470A-HMM binds strongly to actin, dissociates from actin on addition of MgATP, and then only very slowly returns to the strong actin-binding state.

Direct evidence that E470A-HMM hydrolyzes ATP was obtained by determining the relative amounts of ATP and ADP bound to E470A-HMM immediately after removing excess ATP and after 2 h of incubation. By fast performance liquid chromatography (FPLC) analysis, the early time point contained ~95% ATP, whereas the protein incubated for 2 additional hours contained 65% ADP (Fig. 1 B), establishing that the E470A-HMM species that quenched Pyr-actin fluorescence had bound ADP. Therefore, E470A-HMM is capable of ATP hydrolysis, albeit slowly, and the rate of fluorescence decrease is indicative of the rate of a single ATP hydrolysis cycle. This basal MgATPase activity was two orders of magnitude lower than the wild-type molecule

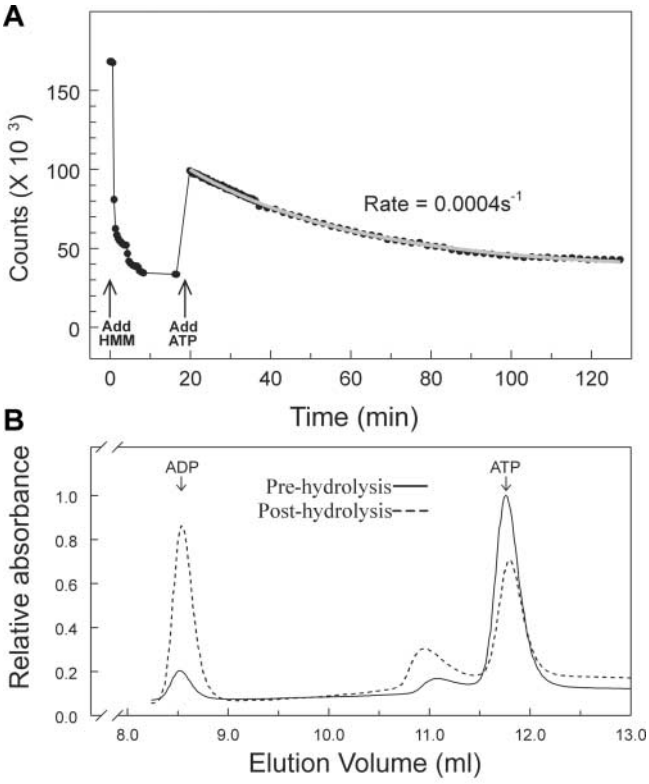

Figure 1. **Hydrolysis of ATP by E470A-HMM.** (A) Time course of pyrene actin fluorescence quenching. 1.6 μM nucleotide-free E470A-HMM was added to 1 μM Pyr-actin at the time noted by the first arrow. Once a new steady-state level of fluorescence was reached, 0.6 μM MgATP was added (second arrow), causing a rapid increase in signal, followed by a slow decay, which was fit to a single exponential (gray line). (B) FPLC chromatograms from samples of E470A-HMM taken immediately (solid line) and 2 h after (dashed line) removal of all free ATP. The absorbance at 260 nm was normalized to that of the largest peak. The identities of the ATP and ADP peaks were established by comparison with trials conducted with pure standards.

(~0.0004 vs. ~0.03 s^{-1}), establishing that E470A-HMM heads exist primarily in a weak actin-binding ATP state.

Homogeneity of the heterodimeric preparation

A homogeneous population of heterodimeric heavy meromyosin (E470A/wt-HMM) was purified (see Materials and methods) as assessed by its ATPase activity and through Western blot analysis. The mutant head is virtually inactive,

Table I. **Ensemble properties of myosin**

Construct	NH_4^+-ATPase	Actin-activated ATPase		Actin velocity[b]
		K_m	V_{max}	
	s^{-1}	μM	s^{-1}	$\mu m s^{-1}$
wt-HMM[a]	24.2 ± 2.8	20 ± 4	2.5 ± 0.2	1.6 ± 0.2 (58)
E470A-HMM[a]	0.01	ND	ND	0.00
E470A/wt-HMM[a]	12.0 ± 0.8	27 ± 7	1.8 ± 0.2	1.5 ± 0.2 (61)
S1-neo	ND	100 ± 44	1.8 ± 0.5	0.5 ± 0.1 (17)

ND, not determined.
[a]Values obtained from Rovner et al. (2003).
[b]Numbers in brackets denote number of filaments sampled.

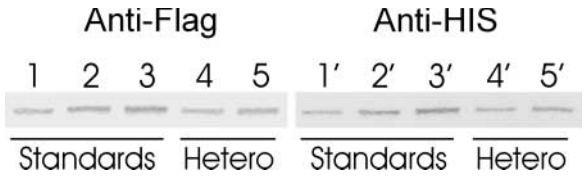

Figure 2. **Western blots of E470A/wt heterodimer.** Left side reacted with anti-Flag antibody M2 (Sigma-Aldrich) and right side reacted with anti-$(His)_6$-tag mAb (Sigma-Aldrich). Lanes 1–3 and 1′-3′ are purified FLAG- and $(His)_6$-labeled HMM standards in loads of 25, 35, and 45 ng, respectively. Lane 4 and lane 5 on both blots are identical samples of the heterodimer containing 35 and 45 ng protein. The amount of Flag- and $(His)_6$-reactive material in the heterodimer was determined by normalization to the staining intensity of the standards.

whereas the wild-type head is fully active, thus the ATPase activity of pure heterodimer should be half that of wt-HMM. To increase the sensitivity of this measurement, we used the NH_4^+-activated ATPase, which has 500-fold higher specific activity than the MgATPase. The activity of E470A-HMM was barely detectable, whereas the activity of E470A/wt-HMM was half that of the wt-HMM (Table I), confirming the homogeneity of the heterodimer (Rovner et al., 2003).

Western blots of the purified E470A/wt-HMM (Fig. 2) provided additional evidence for homogeneity. Identical samples of the heterodimer were probed with FLAG- and $(His)_6$-specific antibodies, and the intensities of the heterodimer bands were normalized by comparison to known quantities of purified FLAG- and $(His)_6$-tagged wt HMMs. This analysis showed that the amounts of FLAG- and $(His)_6$-reactive heavy chain in the heterodimer were equal to within 15%, the limits of measurement errors. This evidence further substantiates our assertion that the heterodimeric preparation is homogeneous.

In vitro motility and actin-activated ATPase

As expected, the E470A-HMM homodimer was unable to move actin filaments in an in vitro motility assay. In contrast, the velocity at which E470A/wt-HMM moved actin was not significantly different from wt-HMM (Table I). If the E470A head acted only as a weak-binding load to movement, one would at best expect a small reduction (~10%) in velocity at equal ratios of the two heads (Warshaw et al., 1990; Harris et al., 1994). For comparison with the double-headed constructs, a single-headed subfragment-1 with neonatal epitope tag at its COOH terminus (S1-neo) was also expressed. This feature allows S1 to be adhered to the nitrocellulose via an antibody to ensure that the head is freely accessible for motility and single-molecule studies. S1-neo moved actin uniformly, but at one-third of the rate obtained with wt-HMM (Table I).

The three constructs were also compared for their actin-activated ATPase activity. When normalized per head, the V_{max} for E470A/wt-HMM was ~75% as great as that for wt-HMM. The actin concentration at half V_{max} (K_m) for these proteins were very similar (Table I). Conversely, S1-neo had a V_{max} similar to that of the heterodimer, but its K_m was about fivefold greater than those of the HMMs (Table I). These data suggest that the presence of a second head enhances the ability of the molecule to interact with actin, even in the presence of ATP.

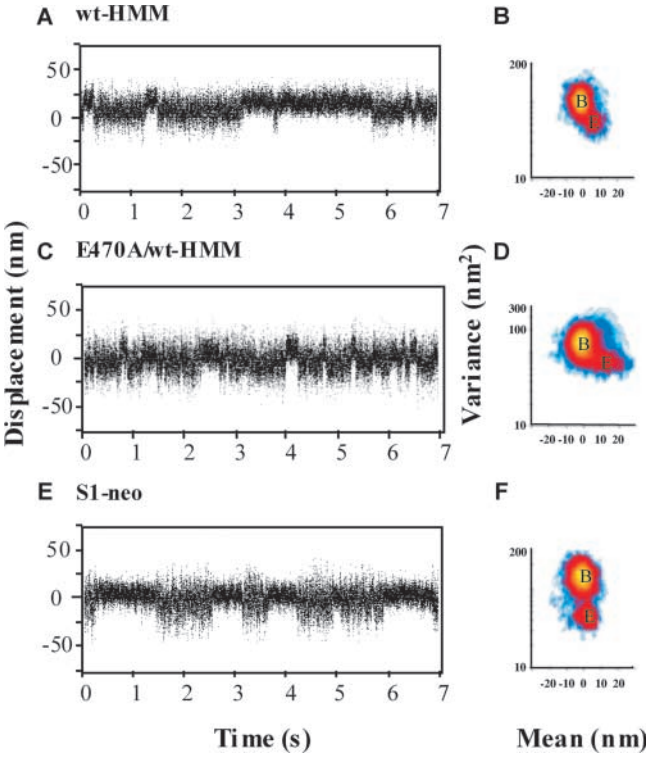

Figure 3. **Single molecule unitary step size determinations.** Representative data traces are shown in A, C, and E for wt-HMM, E470A/wt-HMM, and S1-neo, respectively. Mean-variance histograms are plotted to the right of the original data trace and represent the entire data stream. The histograms are colored in the frequency dimension, with yellow as maximum, blue as minimum, and white as zero. The data streams clearly show the reduction in variance associated with a myosin-binding event; the mean-variance histograms register this as a population distinct from baseline (B) with reduced variance and increased mean position (E). The mean position for S1-neo (E and F) is reduced relative to both E470A/wt-HMM and wt-HMM. The homodimeric E470A-HMM exhibited no distinct strong binding events characteristic of wt-HMM (not depicted), consistent with its inability to displace actin.

Single-molecule studies

The unitary displacement of the heterodimeric E470A/wt-HMM was characterized at the single-molecule level in the optical trap, and compared with wt-HMM and S1-neo (Finer et al., 1994; see also Materials and methods). Representative raw data traces for these three constructs are presented in Fig. 3 (A, C, and E). All three constructs show displacement events that can be visually detected by the reduction in position variance that occurs on myosin strong binding to actin. These data were analyzed using mean variance methods (Patlak, 1993; Guilford et al., 1997), yielding the histograms seen in Fig. 3 (B, D, and F). Each histogram has two clear populations corresponding to baseline (B) when myosin is detached from actin and the displacement events themselves (E), which are separated both by mean position and by variance. Subtracting the mean position of the baseline population from that of the event population yields the myosin step size. Fig. 4 shows the mean step size for each

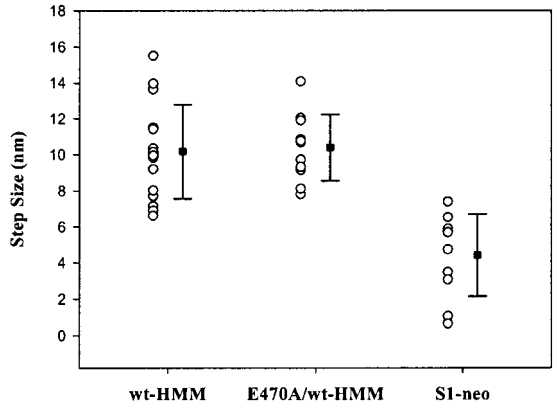

Figure 4. **Myosin step size.** Each circle represents the mean step size obtained for a single myosin molecule in a separate experiment based on mean-variance analysis (Fig. 3). The mean and SDs are indicated by the squares and associated error bars. A detailed summary of these values can be found in Table II.

myosin construct from multiple experiments. A clear difference is evident between the step sizes of wt-HMM and S1-neo (10.2 vs. 4.4 nm; Table II). Remarkably, E470A/wt-HMM, with one compromised head, produced a mean step size of 10.4 nm, almost identical to wt-HMM, but clearly larger than S1-neo.

The step duration (τ_{on}) was also determined from the mean variance analysis (Table II). The values obtained for wt-HMM and E470A/wt-HMM are identical, whereas S1-neo has a longer step duration. Both the step size and τ_{on} data provide strong evidence that the E470A/wt-HMM heterodimer is mechanically indistinguishable from wt-HMM.

Discussion

Muscle myosin IIs and many unconventional myosins have two heads (Mermall et al., 1998). Although both heads are required for unconventional myosin V to achieve processive movement (Purcell et al., 2002; Veigel et al., 2002), the role that each head plays in myosin II motion generation remains unclear. Based on analyses of single- and double-headed myosins in the laser trap, we previously proposed that the displacement generated by a double-headed molecule derives from a single head, and that the magnitude of this displacement is maximized by the presence of the second head (Tyska et al., 1999). Here, we provide evidence in support of this hypothesis by showing that a mutant heterodimer with only one cycling head has a unitary displacement of 10 nm for an average duration of 100 ms, indistinguishable from wt-HMM. Because the mutant head does not have the capacity to generate motion, the step size and average step duration supported by the E470A/wt-HMM heterodimer in the laser trap must originate from the wild-type head. In contrast, the single-headed S1-neo construct also generates displacement from a single head, but the magnitude of this displacement is only half that of wt-HMM. These observations indicate that both heads are required to achieve maximum displacement and that the second head plays a critical role in determining the step size produced by the motion-generating head.

There are several potential mechanisms by which the inactive head could exert its influence on the working head. One possibility is that the step size of the motion-generating head is maximized by virtue of the second head's ability to bind weakly to actin. The electrostatic weak binding of the second head to actin would result in multiple nonstereospecific rapid attachments and detachments, allowing this head to remain in close proximity to actin, and thus exert its influence on the working head (Marston and Taylor, 1980; Geeves and Conibear, 1995). Because no asymmetry exists between the two heads of native myosin, it is likely that either head could become the strong-binding motion-generating head, while the other remains weakly bound. The weak-binding head could then help optimize the orientation of the active head's lever arm relative to the long axis of the actin filament, allowing the entire lever arm displacement to be realized along the actin axis. In support of this hypothesis, the K_m values from actin-activated ATPase assays in our work were much lower for the two double-headed constructs than that of the single-headed S1, suggesting that the second, weakly bound head facilitates the interaction of the molecule with actin. Additionally, there is evidence for an orientational dependence of actin filament velocity in ensembles (Toyoshima et al., 1989; Sellers and Kachar, 1990; Yamada and Wakabayashi, 1993; West et al., 1996), as well as an orientational dependence of the unitary step size for single molecules (Tanaka et al., 1998). The latter experiment measured an approximate 10-nm step size for a single-headed myosin in a rod cofilament only when the rod was parallel to the actin filament. Thus, without the presence of a second head, the 4.4 nm step size generated by the S1-neo construct may be an effective average step size over the range of nonoptimally aligned displacements.

Because the mechanism proposed in the previous paragraph suggests that both heads simultaneously interact with actin, although one less strongly than the other, this interaction may induce strain within the molecule (Margossian and Lowey, 1978). To relieve the potential strain within the molecule due to binding of both heads, some breathing of the coiled-coil S2 segment may occur. This phenomenon was established through experiments where the S2 region was stabilized using a leucine zipper (Lauzon et al., 2001), resulting in a large attenuation of step size. The ability of the coiled-coil to separate may be a feature common to both short-necked conventional and unconventional myosins (e.g., myosin VI) to allow for maximal displacement and processivity, respectively (Rock et al., 2001; Nishikawa et al., 2002).

Table II. **Single molecule properties of myosin**

Construct	Step size[a]	Step duration[b]
	nm	*ms*
wt-HMM	10.2 ± 0.6 (19)	104 ± 13 (15)
S1-neo	4.4 ± 0.7 (10)	189 ± 37 (10)
E470A/wt-HMM	10.4 ± 0.6 (11)	106 ± 10 (9)

Numbers in brackets denote number of single molecules sampled. Errors are given as SEM values.
[a]ANOVA test indicates wt-HMM and S1-neo step sizes are statistically different, whereas wt-HMM and E470A/wt-HMM are not.
[b][ATP] = 10 μm.

An alternative mechanism is that the presence of the second head stabilizes the head–rod junction, minimizing unfavorable orientations and/or conformations of the working head. Coordination between the lever arms (Lidke and Thomas, 2002) could stabilize the head–rod junction of the active head and optimize its stereospecific interaction with actin. Head–head interactions are also possible, such as those observed for smooth muscle HMM during rigor binding to actin (Onishi et al., 1989), or as a means of phosphorylation-dependent regulation (Wendt et al., 1999, 2001; Li and Ikebe, 2003). Although such head–head interactions may be specific to smooth muscle myosin, the unitary displacement of skeletal muscle myosin was also halved on removal of one head (Tyska et al., 1999), suggesting that both smooth and skeletal muscle myosin share some common features that maximize step size.

The data presented here and previously (Tyska et al., 1999) clearly show that double-headed constructs have a twofold larger step size than their single-headed counterparts (~10 vs. ~5 nm). This observation is in contrast to data obtained from other laboratories, who have reported similar step sizes of ~5 nm for S1 and HMM (Molloy et al., 1995; Veigel et al., 1998; Ruff et al., 2001). It is likely that the larger displacement for our HMM constructs compared with other laboratories reflects the mode by which the molecule is attached to the surface. Direct attachment of HMM to nitrocellulose could render one head inactive (Nishizaka et al., 2000), whereas our use of an antibody to raise the HMM from the surface ensures the interaction of both heads with the actin filament (Anson et al., 1996). Indeed, smooth muscle HMM is incapable of supporting in vitro motility when directly applied to a nitrocellulose surface. However, the use of an antibody restores actin filament motility (Trybus and Henry, 1989). Until such time that a skeletal HMM can be expressed or modified to provide an attachment site, the possibility that one of skeletal HMM's heads is adhered to the surface must be considered.

In nature, more subtle variations of our engineered heterodimeric construct exist, when cells coexpress multiple isoforms of the same myosin heavy chain. For example, familial hypertrophic cardiomyopathy (FHC) is a genetic disorder in humans in which point mutations have been identified in the β-cardiac myosin gene (Seidman and Seidman, 1991). Because the mutation occurs most often in a single allele, heterodimeric myosin with one normal and one mutant head will be present. In the FHC R403Q mutant, both heads are capable of hydrolyzing ATP and generating motion, but at substantially different rates (Tyska et al., 2000). Similarly, smooth muscle cells coexpress two isoforms that differ by the presence and absence of a seven-amino acid insert in the surface loop that spans the nucleotide-binding pocket (Kelley et al., 1996; Rovner et al., 1997), and which have twofold different rates of in vitro motility and actin-activated ATPase activity. Our ability to prepare pure populations of such heterodimers will allow us to further probe the functional impact of two heads having different enzymatic and mechanical properties (Rovner et al., 2003).

In summary, for myosin II to generate its maximal step size, two heads are required. For any given displacement event, only one of the two heads moves actin while the other provides a supporting role to optimize the displacement of the active head. The roles for each of the two heads were defined by creating a heterodimer with one cycling and one inactive, weakly binding head. A similar strategy using heterodimers was used when investigating the role that each kinesin head plays in processive movement as well as motion and force generation (Kaseda et al., 2002). When an active head was paired with a head that could only bind microtubules weakly, processivity was retained, although force and velocity were reduced (Kaseda et al., 2002). These results suggest that one active head in a kinesin heterodimer cannot produce maximum force and velocity by itself, in contrast to our results with myosin II. Although our data cannot clarify the exact mechanism by which the second head optimizes the working stroke of the first head, they do make it clear that a double-headed myosin with at least one active head is necessary and sufficient for myosin to express its full mechanical capacity.

Materials and methods

DNA engineering of recombinant baculoviruses

The baculoviral transfer vector pAcSG2 (BD Biosciences) was used to express HMMs with 1175 amino acids of the chicken gizzard heavy chain sequence (Yanagisawa et al., 1987), with either an NH_2-terminal $(His)_6$ tag or a COOH-terminal FLAG tag (Rovner et al., 2003). A COOH-terminal FLAG-tagged HMM mutant with glutamate 470 mutated to alanine was also constructed (E470A-HMM).

A single-headed subfragment-1 (S1-neo) was engineered with 852 amino acids of the wild-type chicken gizzard heavy chain sequence, followed by the last 15 residues of the chicken neonatal myosin rod sequence (VKSREFHKKIEEERS; Moore et al., 1992), and the FLAG epitope for purification. The neonatal sequence provided an epitope tag for monoclonal 5B4 antibody attachment (Lowey et al., 1991) to the nitrocellulose substratum during in vitro motility and single-molecule optical trapping experiments.

Protein expression and purification

Each baculoviral expression construct was transfected and amplified in Sf9 cells by established methods described previously (Trybus, 2000). To express S1-neo, wt-HMM, or E470A-HMM, Sf9 cells were coinfected with the respective FLAG-tagged myosin heavy chain virus and a recombinant virus encoding both the smooth muscle myosin essential and regulatory light chains (Trybus, 2000). For expression of the mutant E470A/wt-HMM, Sf9 cells were coinfected with three viruses encoding the $(His)_6$-tagged wild-type heavy chain, the FLAG-tagged E470A mutant heavy chain, and the dual light chains.

Homodimeric E470A-HMM and S1-neo were purified by affinity chromatography using Sepharose-linked anti-FLAG antibody M2 (Sigma-Aldrich; Trybus, 2000). Heterodimeric E470A/wt-HMM was purified by sequential chromatography on two affinity columns because the HMM expression mixture also contained wt-HMM and E470A-HMM homodimers (for detailed methods see Rovner et al., 2003). The first of these was an anti-FLAG antibody column. The eluate from this column contained both E470A-HMM and E470A/wt-HMM. To purify the heterodimer, this eluate was applied to a Ni^{2+}-charged metal chelate column (Probond; Invitrogen) on the same day. Any nonspecifically bound protein was first removed by washing with a buffer containing 10 mM imidazole. E470A/wt-HMM was then eluted with a buffer containing 300 mM imidazole. Protein was concentrated by dialysis against saturated ammonium sulfate, and the precipitate was collected, resuspended, and dialyzed against a buffer containing 50 mM NaCl, 10 mM Hepes (pH 7.4) at 4°C, 5 mM $MgCl_2$, 1 mM EGTA, and 1 mM DTT. After phosphorylation, glycerol was added to 50%, and the protein was stored at −20°C.

Western blots

A 3–8% acrylamide gradient, Tris-acetate–buffered NuPage® gel (Invitrogen) was run with duplicate lanes of the purified E470A/wt-HMM and multiple identical loadings of wt-HMM that was either FLAG- or $(His)_6$-tagged to generate standard curves. After transfer to nitrocellulose, the portion of

the membrane with FLAG standards was reacted with 0.025 μg/ml anti-FLAG mAb (M2; Sigma-Aldrich). The second membrane portion was incubated with an mAb specific for the $(His)_6$ tag (Sigma-Aldrich) diluted 1:500. Both blots were then treated with HRP-conjugated goat–anti mouse secondary antibody (Bio-Rad Laboratories) diluted 1:2,000. Both filters were developed using DAB in the presence of urea hydrogen peroxide. The developed Western blot was scanned on a flatbed unit, and the amount of material in each band was quantified using Kodak 1D software.

Regulatory light chain phosphorylation

Purified HMMs were phosphorylated by incubation on ice with 0.75 mM free $CaCl_2$, 7.5 μg/ml calmodulin, 1.75 mM MgATP, and 4.5 μg/ml myosin light chain kinase for 3–12 h; the reaction was terminated by addition of 7.5 mM EGTA. The degree of phosphorylation was assessed by glycerol gel electrophoresis with protein samples containing 8 M urea (Perrie and Perry, 1970).

NH_4^+- and actin-activated ATPase activity

NH_4^+-activated ATPase was determined as described previously (Rovner et al., 1995) at 37°C in the following buffer: 400 mM NH_4Cl, 2 mM EDTA, 25 mM Tris Base (pH 8.0) at 37°C, 200 mM sucrose, 1 mM DTT, and 1 mg/ml BSA. ATPase activity in the presence of actin was also measured at 37°C as described previously (Rovner et al., 1995) in a buffer containing 8 mM KCl, 10 mM imidazole-HCl (pH 7.0) at 37°C, 1 mM $MgCl_2$, 1 mM NaN_3, 1 mM DTT, and 2 mM MgATP. Assays were performed at eight actin concentrations over the range of 2.5 to 80 μM; the data were fit by a Michaelis-Menten kinetic model (SlideWrite Plus; Advanced Graphics Software, Inc.) to yield K_m and V_{max} values.

Single turnover analysis of E470A by pyrene fluorescence quenching

To ensure that E470A-HMM was indeed locked in a weak-binding state, we assessed its ability to quench the fluorescence of Pyr-actin. Because this depends on nucleotide hydrolysis and Pi release, this assay provided us with a measure of the mutant's steady-state ATPase activity. Actin was labeled at cysteine 374 with pyrene iodoacetamide as described previously (Joel et al., 2001). Pyrene fluorescence measurements were conducted using a fluorometer (model K2™; ISS, Inc.) at 25°C.

Excess ATP was removed from the solution containing phosphorylated E470A-HMM using a spin column as follows: Sephadex G-50 fine was equilibrated with a buffer containing 100 mM NaCl, 20 mM Hepes (pH 7.5) at 25°C, 5 mM $MgCl_2$, 1 mM EGTA, 1 mM NaN_3, and 1 mM DTT. A 5-ml syringe barrel was filled with this resin, and centrifuged for 6 min at 2,200 rpm in a centrifuge (model TJ-6; Beckman Coulter) to remove buffer. A 200-μl sample of phosphorylated E470A-HMM was added, and the column was spun for 5 min at the same speed. The ATP-free eluate typically contained 75% of the E470A-HMM loaded. The sample was incubated overnight on ice to allow ATP bound at the active site to hydrolyze. On addition to Pyr-actin, fluorescence was quenched. Addition of substoichiometric ATP then caused a rapid fluorescence increase, and the subsequent decay in fluorescence was fit to a single exponential to measure the single ATP turnover rate.

Verification of ATP hydrolysis by E470A-HMM

After excess nucleotide removal from phosphorylated E470A-HMM, the identity of the bound nucleotide was determined immediately and after 2 h of incubation at 25°C as follows: concentrated perchloric acid was added to a final concentration of 5% to denature the protein. The solution was then neutralized to pH 7.0–7.5 with 10 M KOH in 4 M potassium acetate, and the precipitate was removed by centrifugation for 10 min at 14,000 rpm. Using a column (Mono-Q HR 5/5; Amersham Biosciences) equilibrated with 0.5% triethyl ammonium hydrogen bicarbonate, the supernatant was assayed for its relative content of ADP and ATP. The nucleotides in each sample were eluted using a gradient of triethyl ammonium hydrogen bicarbonate from 0.5 to 50%. ADP and ATP peaks were identified by comparison with purified nucleotide standards chromatographed under identical conditions (Fig. 1 B).

In vitro motility

Before motility, any inactive strong-binding heads were removed by high speed centrifugation (350,000 *g* for 25 min) of the expressed construct (150–500 μg/ml) with a twofold molar excess of actin in the presence of 1 mM MgATP in a buffer containing 60 mM KCl, 25 mM imidazole (pH 7.4) at 4°C, 4 mM $MgCl_2$, 1 mM EGTA, and 10 mM DTT. The motility assay was performed at 30°C as described previously (Joel et al., 2001), using the same buffer with additions of a scavenger cocktail (0.25 μg/ml glucose oxidase, 45 μg/ml catalase, 5.75 μg/ml glucose), 1 mM MgATP, and 0.7% methylcellulose. Proteins were diluted to 100 μg/ml before application to the flow cell. HMMs were elevated from the motility surface with antibody S2.2 (Trybus and Henry, 1989), and the S1-neo construct with mAb 5B4 (Lowey et al., 1991).

Optical trap instrumentation

A 2.5-W 1064-nm infrared laser was expanded 10× and digitally chopped between two positions to generate two independent traps using computer-controlled orthogonally orientated acoustic optical deflectors (Neos Technologies, Inc.) cycled at 20 kHz. The beams were subsequently focused to diffraction-limited spots through a 100× objective (1.4 NA Plan Apo IR-enhanced; Nikon) mounted on an inverted microscope (Eclipse TE300; Nikon). Power spectra of 1-μm silica beads in these traps typically reveal a corner frequency below 500 Hz (see stiffness below; but see Molloy et al., 1995; Guilford et al., 1997). Therefore, the frequency of trap interchange is at least two orders of magnitude greater than solution-damped motion of the beads, ensuring stable bead positioning. The brightfield image of the beads was projected onto a quadrant photodetector (QD). This signal, which served as a measure of bead movement, was filtered at 2 kHz followed by 12-bit digitization at 5 kHz, after which it was simultaneously recorded and displayed in real time. Each bead used for experimentation was initially used to calibrate the linear range of the QD; these data were also used to determine the trap stiffness, which from equipartition theory (Dupuis et al., 1997) approximated to 0.03 pN/nm (per trap). Fine microscope stage movement in the x and y dimensions was achieved using a capacitive servo feedback piezoelectric substage (P-731.20; Physik Instrumente) mounted onto the standard microscope support stage. The piezoelectric substage was controlled by computer giving a maximal range of 100 μm^2 with a resolution of 100 nm. Control over substage positioning, number and position of traps, data display, and recording was achieved using custom software designed on a Linux platform running from a dual PII Celeron 400-MHz processor PC.

Standard laser trap assay buffers

Buffers used included myosin buffer, containing 300 mM KCl, 1 mM EGTA, 10 mM DTT, 4 mM $MgCl_2$, and 25 mM imidazole, pH 7.4. Actin buffer was comprised of 10 μM MgATP, 25 mM KCl, 1 mM EGTA, 10 mM DTT, 4 mM $MgCl_2$, 0.25 μg/ml glucose oxidase, 45 μg/ml catalase, 5.75 μg/ml glucose, and 25 mM imidazole, pH 7.4. All experiments were performed at ~20°C.

Laser trap assay

1-μm-diam Silica beads (Bangs Laboratories, Inc.) were coated with NEM-myosin to serve as attachment points for actin filaments by incubating for >30 min at RT in the concentrated (1.4 mg/ml) NEM-myosin solution. Excess NEM-myosin was removed by subsequently washing beads with myosin buffer followed by centrifugation at 10,000 rpm for 5 min; this procedure was then repeated seven times replacing myosin with actin buffer.

Flowcells were constructed as outlined before (Lauzon et al., 1998); however, instead of 100-μm spacers, 125-μm spacers were used to allow a greater period of time to capture the faster falling silica beads used here. In order, the items added to the flowcell were (1) 20 μl 25 μg/ml monoclonal S2.2 antibody (except for S1-neo which required the 5B4 antibody) for 2 min; (2) 100 μl 0.5 mg/ml BSA for >4 min; (3) 30 μl 1 mg/ml myosin for 2 min; (4) 100 μl actin buffer; and (5) 10 μl NEM-bead, tetramethylrhodamine isothiocyanate-labeled actin and actin buffer (containing 10 μM ATP). At this point, the flowcells were rapidly transferred to the microscope and were oil-coupled with the objective. Two traps were created, and a single NEM-myosin coated silica bead captured in each. The stage was then maneuvered to tether the ends of a free actin filament to each bead. The actin was pretensioned to at least 4 pN by adjusting the separation of the traps. This bead–actin–bead assembly was lowered onto a bead sparsely coated with myosin attached to the flowcell surface, and the photodetector output was recorded. Using low protein concentrations (1 μg/ml), it was possible to increase the probability that only a single myosin molecule could interact with the actin filament.

Myosin interactions with actin lead to a signature drop in bead position variance due to addition of myosin stiffness to the system (Dupuis et al., 1997; Veigel et al., 1998). In addition, a change in the mean position of the QD output corresponding to the unitary displacement was measured. These data were analyzed using the mean-variance (MV) method (Patlak, 1993; Guilford et al., 1997). This automated analysis plots a histogram of the mean position versus the variance for a specified window width that runs over the complete data stream. Altering the window size used during

MV analysis enables one to determine mean step durations. Such changes in window width affect the relative volumes of baseline and event populations; the latter exhibits an exponential relationship with the window size. The exponent of a fit to these data reveal the step duration.

We thank Dr. J. Moore, S. Work, and D. Gaffney II for their considerable help in testing and software development for the optical trap; Drs. J. Baker, J. Moore, and S. Lowey for helpful discussions; Ms. A. Federico, Ms. C. Brosseau, and Ms. A. Armstrong for their expert technical help; Ms. V. Turner for critical reading of portions of this manuscript; and Mr. Q. Wan for help in determining by FPLC the identity of the nucleotide bound to the mutant.

This work was supported by funds from the National Institutes of Health (AR47906 and HL59408) to K.M. Trybus, D.M. Warshaw, and J.B. Patlak.

Submitted: 4 April 2003
Accepted: 18 June 2003

References

Anson, M., M.A. Geeves, S.E. Kurzawa, and D.J. Manstein. 1996. Myosin motors with artificial lever arms. *EMBO J.* 15:6069–6074.

Baker, J.E., I. Brust-Mascher, S. Ramachandran, L.E. LaConte, and D.D. Thomas. 1998. A large and distinct rotation of the myosin light chain domain occurs upon muscle contraction. *Proc. Natl. Acad. Sci. USA.* 95:2944–2949.

Conibear, P.B., and M.A. Geeves. 1998. Cooperativity between the two heads of rabbit skeletal muscle heavy meromyosin in binding to actin. *Biophys. J.* 75: 926–937.

Cooke, R., and K.E. Franks. 1978. Generation of force by single-headed myosin. *J. Mol. Biol.* 120:361–373.

Corrie, J.E., B.D. Brandmeier, R.E. Ferguson, D.R. Trentham, J. Kendrick-Jones, S.C. Hopkins, U.A. van der Heide, Y.E. Goldman, C. Sabido-David, R.E. Dale, et al. 1999. Dynamic measurement of myosin light-chain-domain tilt and twist in muscle contraction. *Nature*. 400:425–430.

Cremo, C.R., J.R. Sellers, and K.C. Facemyer. 1995. Two heads are required for phosphorylation-dependent regulation of smooth muscle myosin. *J. Biol. Chem.* 270:2171–2175.

Criddle, A.H., M.A. Geeves, and T. Jeffries. 1985. The use of actin labelled with N-(1-pyrenyl)iodoacetamide to study the interaction of actin with myosin subfragments and troponin/tropomyosin. *Biochem. J.* 232:343–349.

Dominguez, R., Y. Freyzon, K.M. Trybus, and C. Cohen. 1998. Crystal structure of a vertebrate smooth muscle myosin motor domain and its complex with the essential light chain: visualization of the pre-power stroke state. *Cell.* 94: 559–571.

Dupuis, D.E., W.H. Guilford, J. Wu, and D.M. Warshaw. 1997. Actin filament mechanics in the laser trap. *J. Muscle Res. Cell Motil.* 18:17–30.

Finer, J.T., R.M. Simmons, and J.A. Spudich. 1994. Single myosin molecule mechanics: piconewton forces and nanometre steps. *Nature.* 368:113–119.

Geeves, M.A., and P.B. Conibear. 1995. The role of three-state docking of myosin S1 with actin in force generation. *Biophys. J.* 68:194S–199S.

Guilford, W.H., D.E. Dupuis, G. Kennedy, J. Wu, J.B. Patlak, and D.M. Warshaw. 1997. Smooth muscle and skeletal muscle myosins produce similar unitary forces and displacements in the laser trap. *Biophys. J.* 72:1006–1021.

Harada, Y., A. Noguchi, A. Kishino, and T. Yanagida. 1987. Sliding movement of single actin filaments on one-headed myosin filaments. *Nature.* 326:805–808.

Harris, D.E., S.S. Work, R.K. Wright, N.R. Alpert, and D.M. Warshaw. 1994. Smooth, cardiac and skeletal muscle myosin force and motion generation assessed by cross-bridge mechanical interactions in vitro. *J. Muscle Res. Cell Motil.* 15:11–19.

Houdusse, A., A.G. Szent-Gyorgyi, and C. Cohen. 2000. Three conformational states of scallop myosin S1. *Proc. Natl. Acad. Sci. USA.* 97:11238–11243.

Huxley, H.E., and M. Kress. 1985. Crossbridge behaviour during muscle contraction. *J. Muscle Res. Cell Motil.* 6:153–161.

Ito, K., X. Liu, E. Katayama, and T.Q. Uyeda. 1999. Cooperativity between two heads of dictyostelium myosin II in in vitro motility and ATP hydrolysis. *Biophys. J.* 76:985–992.

Joel, P.B., K.M. Trybus, and H.L. Sweeney. 2001. Two conserved lysines at the 50/20-kDa junction of myosin are necessary for triggering actin activation. *J. Biol. Chem.* 276:2998–3003.

Kaseda, K., H. Higuchi, and K. Hirose. 2002. Coordination of kinesin's two heads studied with mutant heterodimers. *Proc. Natl. Acad. Sci. USA*. 99:16058–16063. First published on November 25, 2002; 10.1073/pnas.252409199.

Katayama, E. 1998. Quick-freeze deep-etch electron microscopy of the actin-heavy meromyosin complex during the in vitro motility assay. *J. Mol. Biol.* 278: 349–367.

Kelley, C.A., J.R. Sellers, D.L. Gard, D. Bui, R.S. Adelstein, and I.C. Baines. 1996. *Xenopus* nonmuscle myosin heavy chain isoforms have different subcellular localizations and enzymatic activities. *J. Cell Biol.* 134:675–687.

Kojima, S., K. Fujiwara, and H. Onishi. 1999. SH1 (cysteine 717) of smooth muscle myosin: its role in motor function. *Biochemistry.* 38:11670–11676.

Lauzon, A.M., M.J. Tyska, A.S. Rovner, Y. Freyzon, D.M. Warshaw, and K.M. Trybus. 1998. A 7-amino-acid insert in the heavy chain nucleotide binding loop alters the kinetics of smooth muscle myosin in the laser trap. *J. Muscle Res. Cell Motil.* 19:825–837.

Lauzon, A.M., P.M. Fagnant, D.M. Warshaw, and K.M. Trybus. 2001. Coiled-coil unwinding at the smooth muscle myosin head-rod junction is required for optimal mechanical performance. *Biophys. J.* 80:1900–1904.

Li, X.D., and M. Ikebe. 2003. Two functional heads are required for full activation of smooth muscle myosin. *J. Biol. Chem.* In press.

Lidke, D.S., and D.D. Thomas. 2002. Coordination of the two heads of myosin during muscle contraction. *Proc. Natl. Acad. Sci. USA.* 99:14801–14806.

Lowey, S., G.S. Waller, and E. Bandman. 1991. Neonatal and adult myosin heavy chains form homodimers during avian skeletal muscle development. *J. Cell Biol.* 113:303–310.

Margossian, S.S., and S. Lowey. 1973. Substructure of the myosin molecule. IV. Interactions of myosin and its subfragments with adenosine triphosphate and F-actin. *J. Mol. Biol.* 74:313–330.

Margossian, S.S., and S. Lowey. 1978. Interaction of myosin subfragments with F-actin. *Biochemistry.* 17:5431–5439.

Marston, S.B., and E.W. Taylor. 1980. Comparison of the myosin and actomyosin ATPase mechanisms of the four types of vertebrate muscles. *J. Mol. Biol.* 139:573–600.

Mermall, V., P.L. Post, and M.S. Mooseker. 1998. Unconventional myosins in cell movement, membrane traffic, and signal transduction. *Science.* 279:527–533.

Molloy, J.E., J.E. Burns, J. Kendrick-Jones, R.T. Tregear, and D.C. White. 1995. Movement and force produced by a single myosin head. *Nature.* 378:209–212.

Moore, L.A., M.J. Arrizubieta, W.E. Tidyman, L.A. Herman, and E. Bandman. 1992. Analysis of the chicken fast myosin heavy chain family. Localization of isoform-specific antibody epitopes and regions of divergence. *J. Mol. Biol.* 225:1143–1151.

Nishikawa, S., K. Homma, Y. Komori, M. Iwaki, T. Wazawa, I.A. Hikikoshi, J. Saito, R. Ikebe, E. Katayama, T. Yanagida, and M. Ikebe. 2002. Class VI myosin moves processively along actin filaments backward with large steps. *Biochem. Biophys. Res. Commun.* 290:311–317.

Nishizaka, T., R. Seo, H. Tadakuma, K. Kinosita, Jr., and S. Ishiwata. 2000. Characterization of single actomyosin rigor bonds: load dependence of lifetime and mechanical properties. *Biophys. J.* 79:962–974.

Onishi, H., T. Maita, G. Matsuda, and K. Fujiwara. 1989. Evidence for the association between two myosin heads in rigor acto-smooth muscle heavy meromyosin. *Biochemistry.* 28:1898–1904.

Onishi, H., S. Kojima, K. Katoh, K. Fujiwara, H.M. Martinez, and M.F. Morales. 1998a. Functional transitions in myosin: formation of a critical salt-bridge and transmission of effect to the sensitive tryptophan. *Proc. Natl. Acad. Sci. USA.* 95:6653–6658.

Onishi, H., M.F. Morales, S. Kojima, K. Katoh, and K. Fujiwara. 1998b. Smooth muscle myosin. Amino acid residues responsible for the hydrolysis of ATP. *Adv. Exp. Med. Biol.* 453:99–103.

Patlak, J.B. 1993. Measuring kinetics of complex single ion channel data using mean-variance histograms. *Biophys. J.* 65:29–42.

Perrie, W.T., and S.V. Perry. 1970. An electrophoretic study of the low-molecular-weight components of myosin. *Biochem. J.* 119:31–38.

Purcell, T.J., C. Morris, J.A. Spudich, and H.L. Sweeney. 2002. Role of the lever arm in the processive stepping of myosin V. *Proc. Natl. Acad. Sci. USA.* 99: 14159–14164.

Rayment, I., W.R. Rypniewski, K. Schmidt-Base, R. Smith, D.R. Tomchick, M.M. Benning, D.A. Winkelmann, G. Wesenberg, and H.M. Holden. 1993. Three-dimensional structure of myosin subfragment-1: a molecular motor. *Science.* 261:50–58.

Rock, R.S., S.E. Rice, A.L. Wells, T.J. Purcell, J.A. Spudich, and H.L. Sweeney. 2001. Myosin VI is a processive motor with a large step size. *Proc. Natl. Acad. Sci. USA.* 98:13655–13659.

Rovner, A.S., Y. Freyzon, and K.M. Trybus. 1995. Chimeric substitutions of the actin-binding loop activate dephosphorylated but not phosphorylated smooth muscle heavy meromyosin. *J. Biol. Chem.* 270:30260–30263.

Rovner, A.S., Y. Freyzon, and K.M. Trybus. 1997. An insert in the motor domain determines the functional properties of expressed smooth muscle myosin isoforms. *J. Muscle Res. Cell Motil.* 18:103–110.

Rovner, A.S., P.M. Fagnant, and K.M. Trybus. 2003. The two heads of smooth muscle myosin are enzymatically independent but mechanically interactive. *J. Biol. Chem.* 278:26938–26945. First published on April 21, 2003; 10.1074/jbc.M303122200.

Ruff, C., M. Furch, B. Brenner, D.J. Manstein, and E. Meyhofer. 2001. Single-molecule tracking of myosins with genetically engineered amplifier domains. *Nat. Struct. Biol.* 8:226–229.

Sasaki, N., T. Shimada, and K. Sutoh. 1998. Mutational analysis of the switch II loop of *Dictyostelium* myosin II. *J. Biol. Chem.* 273:20334–20340.

Seidman, C.E., and J.G. Seidman. 1991. Mutations in cardiac myosin heavy chain genes cause familial hypertrophic cardiomyopathy. *Mol. Biol. Med.* 8:159–166.

Sellers, J.R., and B. Kachar. 1990. Polarity and velocity of sliding filaments: control of direction by actin and of speed by myosin. *Science.* 249:406–408.

Shih, W.M., and J.A. Spudich. 2001. The myosin relay helix to converter interface remains intact throughout the actomyosin ATPase cycle. *J. Biol. Chem.* 276: 19491–19494.

Suzuki, Y., T. Yasunaga, R. Ohkura, T. Wakabayashi, and K. Sutoh. 1998. Swing of the lever arm of a myosin motor at the isomerization and phosphate-release steps. *Nature.* 396:380–383.

Tanaka, H., A. Ishijima, M. Honda, K. Saito, and T. Yanagida. 1998. Orientation dependence of displacements by a single one-headed myosin relative to the actin filament. *Biophys. J.* 75:1886–1894.

Toyoshima, Y.Y., S.J. Kron, E.M. McNally, K.R. Niebling, C. Toyoshima, and J.A. Spudich. 1987. Myosin subfragment-1 is sufficient to move actin filaments in vitro. *Nature.* 328:536–539.

Toyoshima, Y.Y., C. Toyoshima, and J.A. Spudich. 1989. Bidirectional movement of actin filaments along tracks of myosin heads. *Nature.* 341:154–156.

Trybus, K.M. 2000. Biochemical studies of myosin. *Methods.* 22:327–335.

Trybus, K.M., and L. Henry. 1989. Monoclonal antibodies detect and stabilize conformational states of smooth muscle myosin. *J. Cell Biol.* 109:2879–2886.

Tyska, M.J., D.E. Dupuis, W.H. Guilford, J.B. Patlak, G.S. Waller, K.M. Trybus, D.M. Warshaw, and S. Lowey. 1999. Two heads of myosin are better than one for generating force and motion. *Proc. Natl. Acad. Sci. USA.* 96:4402–4407.

Tyska, M.J., E. Hayes, M. Giewat, C.E. Seidman, J.G. Seidman, and D.M. Warshaw. 2000. Single-molecule mechanics of R403Q cardiac myosin isolated from the mouse model of familial hypertrophic cardiomyopathy. *Circ. Res.* 86:737–744.

Uyeda, T.Q., P.D. Abramson, and J.A. Spudich. 1996. The neck region of the myosin motor domain acts as a lever arm to generate movement. *Proc. Natl. Acad. Sci. USA.* 93:4459–4464.

Veigel, C., M.L. Bartoo, D.C. White, J.C. Sparrow, and J.E. Molloy. 1998. The stiffness of rabbit skeletal actomyosin cross-bridges determined with an optical tweezers transducer. *Biophys. J.* 75:1424–1438.

Veigel, C., F. Wang, M.L. Bartoo, J.R. Sellers, and J.E. Molloy. 2002. The gated gait of the processive molecular motor, myosin V. *Nat. Cell Biol.* 4:59–65.

Warshaw, D.M., J.M. Desrosiers, S.S. Work, and K.M. Trybus. 1990. Smooth muscle myosin cross-bridge interactions modulate actin filament sliding velocity in vitro. *J. Cell Biol.* 111:453–463.

Wendt, T., D. Taylor, T. Messier, K.M. Trybus, and K.A. Taylor. 1999. Visualization of head-head interactions in the inhibited state of smooth muscle myosin. *J. Cell Biol.* 147:1385–1390.

Wendt, T., D. Taylor, K.M. Trybus, and K. Taylor. 2001. Three-dimensional image reconstruction of dephosphorylated smooth muscle heavy meromyosin reveals asymmetry in the interaction between myosin heads and placement of subfragment 2. *Proc. Natl. Acad. Sci. USA.* 98:4361–4366.

West, J.M., H. Higuchi, A. Ishijima, and T. Yanagida. 1996. Modification of the bi-directional sliding movement of actin filaments along native thick filaments isolated from a clam. *J. Muscle Res. Cell Motil.* 17:637–646.

Yamada, A., and T. Wakabayashi. 1993. Movement of actin away from the center of reconstituted rabbit myosin filament is slower than in the opposite direction. *Biophys. J.* 64:565–569.

Yanagisawa, M., Y. Hamada, Y. Katsuragawa, M. Imamura, T. Mikawa, and T. Masaki. 1987. Complete primary structure of vertebrate smooth muscle myosin heavy chain deduced from its complementary DNA sequence. Implications on topography and function of myosin. *J. Mol. Biol.* 198:143–157.